VOLUME 71, NUMBER 5

JOC Articles

MARCH 3, 2006

Ruthenium Tetraoxide Oxidations of Alkanes: DFT Calculations of Barrier Heights and Kinetic Isotope Effects

Markus Drees and Thomas Strassner*

Institut für Organische Chemie, Technische Universität Dresden, 01062 Dresden, Germany

thomas.strassner@chemie.tu-dresden.de

Received July 21, 2005

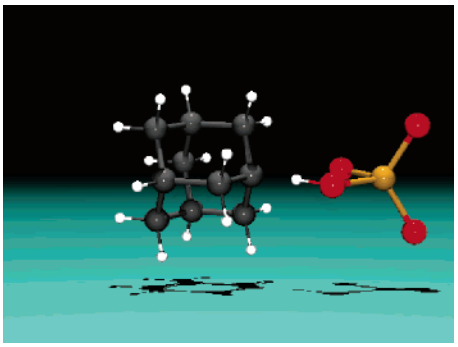

The oxidation of C−H and C−C bonds by metal−oxo compounds is of general interest. We studied the RuO_4-mediated catalytic oxidation of several cycloalkanes such as adamantane and *cis*- and *trans*-decalin as well as methane. B3LYP/6-31G(d) calculations on the experimentally proposed (3+2) mechanism are in good agreement with known experimental results. Comparison of experimental and theoretical kinetic isotope effects confirms the proposed mechanism. Besides RuO_4, we also looked at $RuO_4(OH)^-$ as a potential active species to account for ruthenium tetraoxide oxidations under strong basic conditions.

Introduction

Ruthenium tetraoxide is a powerful oxidant, capable of oxidizing C−H as well as C−C bonds with different hybridizations ($sp-sp^3$).[1,2] We are interested in metal−oxo compounds that are capable of conducting oxidative functionalizations of saturated hydrocarbons. In 1953, Djerassi and Engle[3] introduced ruthenium tetraoxide as an oxidant in the field of organic synthesis, but had to overcome the danger of explosions by using halogenated solvents. Nowadays ruthenium tetraoxide is prepared in situ by oxidizing ruthenium precursors in lower oxidation states (such as $RuCl_3$ or RuO_2) to Ru(VIII). The most popular preparation is known as the "Sharpless condition":[4] $RuCl_3$ is oxidized by periodate (IO_4^-) in a biphasic solution (solvent mixture of water, CCl_4, and acetonitrile), producing Ru(VIII)oxide RuO_4 as the active species in the oxidation chemistry.

Alkane oxidations by ruthenium tetraoxide were thoroughly investigated by Waegell[5−8] and Bakke.[9−14] The French group

* Phone: +49 +351 463 38 571. Fax: +49 +351 463 39 679.

(1) Sica, D. *Recent Res. Dev. Org. Chem.* **2003**, *7*, 105−127.
(2) Frunzke, J.; Loschen, C.; Frenking, G. *J. Am. Chem. Soc.* **2004**, *126*, 3642−3652.
(3) Djerassi, C.; Engle, R. R. *J. Am. Chem. Soc.* **1953**, *75*, 3838−3840.
(4) Carlsen, P. H. J.; Katsuki, T.; Martin, V. S.; Sharpless, K. B. *J. Org. Chem.* **1981**, *46*, 3936−3938.
(5) Coudret, J. L.; Waegell, B. *Inorg. Chim. Acta* **1994**, *222*, 115−122.
(6) Tenaglia, A.; Terranova, E.; Waegell, B. *J. Org. Chem.* **1992**, *57*, 5523−5528.
(7) Tenaglia, A.; Terranova, E.; Waegell, B. *Chem. Commun.* **1990**, 1344−1345.
(8) Tenaglia, A.; Terranova, E.; Waegell, B. *Tetrahedron Lett.* **1989**, *30*, 5271−5274.
(9) Bakke, J. M.; Froehaug, A. E. *J. Phys. Org. Chem.* **1996**, *9*, 507−513.

10.1021/jo051521d CCC: $33.50
Published on Web 11/05/2005

(Waegell) focused on the isolation of oxidation products in mainly oligocyclic systems, whereas the Norwegian group (Bakke) investigated mechanistic questions by using kinetic isotope effects (KIE) and solvent and substituent effects. Bakke et al.[14] postulated the first mechanism in 1986, suggesting the formation of ionic species during the reaction (eq 1).

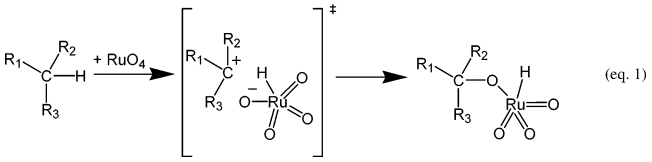

(eq. 1)

Following the general discussion about the oxidation mechanism of metal−oxo compounds in the late 80s and early 90s, Waegell[8] proposed a cyclic (2+2) addition mechanism, shown below (eq 2).

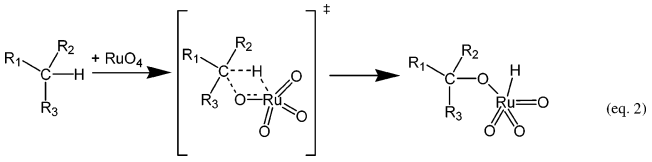

(eq. 2)

In 1992 Bakke addressed both mechanistic proposals,[12] but his work on substituent effects did not end the mechanistic discussion. On the basis of the observed larger kinetic isotope effect, they confirmed their initially proposed mechanism according to eq 1.

During the same year, Waegell[6] again discarded the ionic mechanism, and introduced another pathway by proposing a concerted but asynchronous (3+2) addition reaction via a five-membered ring as the rate-determining transition state (eq 3).

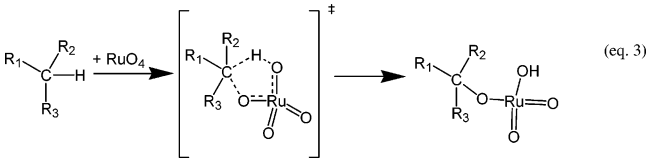

(eq. 3)

Bakke reinvestigated the reaction kinetics in different solvents.[11] The absence of solvent effects on the reaction rate and the observed retention of configuration in the products seem to disprove an ionic mechanism; they are in better agreement with a concerted mechanism.

The Bakke group also changed the interpretation of their KIE measurements.[9,10] Although they explained their experimentally observed large KIE in the earlier study[12] with an eventually observed secondary KIE (typical for ionic mechanisms), in their later study,[9] they ruled out secondary KIEs by the choice of deuterated substrates. They still observed a large (primary) KIE of 5−7, but explained it by a concerted (3+2) mechanism, together with solvent effects.

SCHEME 1. Adamantane (1 or AD), *cis*- (2 or CD) and *trans*-Decalin (3 or TD), and Methane (4)

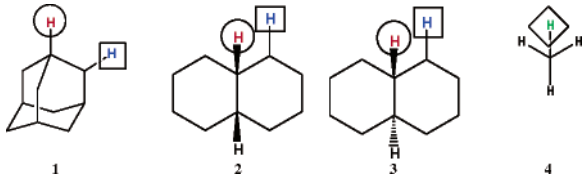

Our research program on the conversion of methane to methanol,[15−18] and the interest in metal−oxo compounds and their oxidation reactions,[19−27] prompted us to study the different reaction mechanisms of alkane oxidations. The combination of experimental and theoretical KIEs has recently proven to be a very successful method for the elucidation of reaction mechanisms.[19,28−33] To apply this technique for the RuO_4-catalyzed oxidation of alkanes, we computed the oxidation of selected alkanes for which experimental KIE data are available in the literature.[9,10] Knowledge of the structures and relative energies of possible transition states has shown to be helpful in pointing the way to the correct mechanism.[34] Especially in combination with experimental observations such as KIEs, theory can provide valuable insight into the reaction mechanism.

Here, we present DFT calculations on transition states of the catalytic ruthenium tetraoxide C−H activation of adamantane and *cis*- and *trans*-decalin, and compare these values to experimentally determined activation enthalpies and free energies. A related oxidant, osmium tetraoxide (OsO_4), has recently been found to be very sensitive to the pH value. Mayer has shown for the oxidation of dihydrogen[35] and isobutane[36] that

(10) Bakke, J. M.; Froehaug, A. E. *J. Phys. Org. Chem.* **1996**, *9*, 310−318.
(11) Bakke, J. M.; Froehaug, A. E. *Acta Chem. Scand.* **1994**, *48*, 160−164.
(12) Bakke, J. M.; Bethell, D. *Acta Chem. Scand.* **1992**, *46*, 644−649.
(13) Bakke, J. M.; Braenden, J. E. *Acta Chem. Scand.* **1991**, *45*, 418−423.
(14) Bakke, J. M.; Lundquist, M. *Acta Chem. Scand. B* **1986**, *B40*, 430−433.
(15) Muehlhofer, M.; Strassner, T.; Herrmann, W. A. *Angew. Chem., Int. Ed.* **2002**, *41*, 1745−1747.
(16) Muehlhofer, M.; Strassner, T.; Herdtweck, E.; Herrmann, W. A. *J. Organomet. Chem.* **2002**, *660*, 121−126.
(17) Herdtweck, E.; Muehlhofer, M.; Strassner, T. *Acta Crystallogr., Sect. E* **2003**, *E59*, m970−m971.
(18) Strassner, T.; Muehlhofer, M.; Zeller, A.; Herdtweck, E.; Herrmann, W. A. *J. Organomet. Chem.* **2004**, *689*, 1418−1424.
(19) DelMonte, A. J.; Haller, J.; Houk, K. N.; Sharpless, K. B.; Singleton, D. A.; Strassner, T.; Thomas, A. A. *J. Am. Chem. Soc.* **1997**, *119*, 9907−9908.
(20) Houk, K. N.; Strassner, T. *J. Org. Chem.* **1999**, *64*, 800−802.
(21) Strassner, T.; Houk, K. N. *J. Am. Chem. Soc.* **2000**, *122*, 7821−7822.
(22) Strassner, T.; Busold, M. *J. Org. Chem.* **2001**, *66*, 672−676.
(23) Collman, J. P.; Slaughter, L. M.; Eberspacher, T. A.; Strassner, T.; Brauman, J. I. *Inorg. Chem.* **2001**, *40*, 6272−6280.
(24) Strassner, T.; Muehlhofer, M.; Grasser, S. *J. Organomet. Chem.* **2002**, *641*, 121−125.
(25) Strassner, T. *Adv. Phys. Org. Chem.* **2003**, *38*, 131−160.
(26) Strassner, T.; Busold, M. *J. Phys. Chem. A* **2004**, *108*, 4455−4458.
(27) Drees, M.; Strassner, T. *J. Mol. Struct.: THEOCHEM* **2004**, *671*, 197−204.
(28) Saettel, N. J.; Wiest, O.; Singleton, D. A.; Meyer, M. P. *J. Am. Chem. Soc.* **2002**, *124*, 11552−11559.
(29) Meyer, M. P.; DelMonte, A. J.; Singleton, D. A. *J. Am. Chem. Soc.* **1999**, *121*, 10865−10874.
(30) Singleton, D. A.; Merrigan, S. R.; Beno, B. R.; Houk, K. N. *Tetrahedron Lett.* **1999**, *40*, 5817−5821.
(31) Keating, A. E.; Merrigan, S. R.; Singleton, D. A.; Houk, K. N. *J. Am. Chem. Soc.* **1999**, *121*, 3933−3938.
(32) Singleton, D. A.; Merrigan, S. R.; Liu, J.; Houk, K. N. *J. Am. Chem. Soc.* **1997**, *119*, 3385−3386.
(33) Beno, B. R.; Houk, K. N.; Singleton, D. A. *J. Am. Chem. Soc.* **1996**, *118*, 9984−9985.
(34) Torrent, M.; Sola, M.; Frenking, G. *Chem. Rev.* **2000**, *100*, 439−493.
(35) Dehestani, A.; Lam, W. H.; Hrovat, D. A.; Davidson, E. R.; Borden, W. T.; Mayer, J. M. *J. Am. Chem. Soc.* **2005**, *127*, 3423−3432.
(36) Bales, B. C.; Brown, P.; Dehestani, A.; Mayer, J. M. *J. Am. Chem. Soc.* **2005**, *127*, 2832−2833.

TABLE 1. Comparison of Free Enthalpies ($\Delta H^{\ddagger}$) and Free Energies ($\Delta G^{\ddagger}$) for the (3+2) Transition States (in kcal/mol) for Adamantane (AD), *cis*-Decalin (CD), *trans*-Decalin (TD), and Methane (CH_4)

	$\Delta H^{\ddagger gas}_{calc}$	$\Delta G^{\ddagger gas}_{calc}$	$\Delta G^{\ddagger AC}_{calc}$	$\Delta G^{\ddagger AN}_{calc}$	$\Delta H^{\ddagger AN}_{exp}$	$\Delta G^{\ddagger AN}_{exp}$	$\Delta H^{\ddagger AC}_{exp}$	$\Delta G^{\ddagger AC}_{exp}$
TS1a (AD-○)	13.9	23.6	20.0	19.9	14.8	22.3	14.0	20.1
TS1b (AD-□)	16.4	26.6	23.9	23.5				
TS2a (CD-○)	13.8	24.1	21.7	22.7	14.7	22.7	12.3	20.2
TS2b (CD-□)	16.5	26.1	23.1	22.9				
TS3a (TD-○)	16.1	25.7	23.3	23.6	16.2	23.6		
TS3b (TD-□)	15.8	25.3	22.7	22.3				
TS4 (CH_4-◇)	26.3	34.6						

TABLE 2. Comparison of Calculated and Experimental KIE Values

	KIE_{calc}	$KIE^{acetone/water}_{exp}$	$KIE^{CCl_4/CH_3CN/H_2O}_{exp}$	used isotopomer
TS1a (AD-○)	6.0	7.8	4.8	d^4-adamantane
TS1b (AD-□)	5.5			d^1-adamantane
TS2a (CD-○)	5.0	6.8	4.8	d^{18}-*cis*-decalin
TS2b (CD-□)	4.4			d^{18}-*cis*-decalin
TS3a (TD-○)	5.6			d^{18}-*trans*-decalin
TS3b (TD-□)	4.6			d^{18}-*trans*-decalin
TS4 (CH_4-◇)	5.1			CD_4

TABLE 3. Free Enthalpies and Energies of Intermediates (kcal/mol)

	ΔH^{gas}_{calc}	ΔG^{gas}_{calc}
IM1a (AD-○)	−46.0	−35.8
IM1b (AD-□)	−36.9	−26.7
IM2a (CD-○)	−36.5	−25.8
IM2b (CD-□)	−36.3	−26.1
IM3a (TD-○)	−43.0	−32.4
IM3b (TD-□)	−42.0	−32.1
IM4 (CH_4-◇)	−27.3	−19.5

TABLE 4. Relative Energies of Transition States and Intermediates and KIEs for the $RuO_4(OH)^-$ Oxidation

	$\Delta H^{\ddagger gas}_{calc}$	$\Delta G^{\ddagger gas}_{calc}$	ΔH^{IMgas}_{calc}	ΔG^{IMgas}_{calc}	KIE_{calc}
TS/IM5a (AD-○)	11.6	23.5	−60.6	−47.4	6.2
TS/IM5b (AD-□)	16.2	27.8	−61.3	−48.8	5.5
TS/IM6a (CD-○)	10.5	22.7	−59.4	−45.9	5.8
TS/IM6b (CD-□)	14.3	26.6	−60.7	−47.7	6.0
TS/IM7a (TD-○)	11.2	23.2	−58.4	−46.3	5.9
TS/IM7b (TD-□)	11.8	23.5	−57.4	−45.5	5.6
TS8/IM (CH_4-◇)	18.4	28.4	−50.5	−40.4	5.6

the pH dependency makes it necessary to also look at anionic complexes such as $RuO_4(OH)^-$ as potential catalytic species under basic conditions.

Computational Details

All calculations were performed with GAUSSIAN-03,[37] using the density functional/Hartree−Fock hybrid model Becke3LYP[38−41] and the split valence double-ζ (DZ) basis set 6-31G(d)[42] for C, H, and O. The Stuttgart/Dresden 1997 ECP[43,44] was used for Ru; it is thoroughly tested, and has proven to be the best choice in the case of the RuO_4-catalyzed alkene oxidation.[27] No symmetry or internal coordinate constraints were applied during optimizations. All reported intermediates were verified as being true minima by the absence of negative eigenvalues in the vibrational frequency analysis. Transition-state structures (indicated by TS) were located using the Berny algorithm[45] until the Hessian matrix had only one imaginary eigenvalue. The identities of all transition states were confirmed by IRC calculations, and by animating the negative eigenvector coordinate with MOLDEN[46] and GaussView.

The results shown are for the singlet potential energy hypersurface (PES), as triplet species have been found to be higher in energy. Approximate free energies (Δ*G*) and enthalpies (Δ*H*) were obtained through thermochemical analysis of frequency calculations, using the thermal correction to Gibbs free energy as reported by GAUSSIAN-03. This takes into account zero-point effects, thermal enthalpy corrections, and entropy. All energies reported in this paper, unless otherwise noted, are free energies or enthalpies at 298 K, using unscaled frequencies. All transition states are maxima on the electronic potential energy surface (PES), which may not correspond to maxima on the free energy surface. Solvation corrections were applied using the PCM model[47] as implemented in GAUSSIAN-03.

Theoretical KIE values were obtained by using the program package QUIVER-C,[48] a code very similar to QUIVER,[49] but ported to C++ to enable the calculation of larger numbers of atoms, which is restricted in the original version. This program calculates Biegeleisen−Mayer coefficients and partition functions of different isotopomers from the corresponding formatted GAUSSIAN-03 checkpoint file, using a scaling factor of 0.98 for the basis set used.

Results and Discussion

We calculated the transition states for the activation of tertiary (○) and secondary (□) hydrogen bonds of adamantane (**1**), *cis*-(**2**) and *trans*-decalin (**3**), as well as the transition state for methane (**4**) activation (◇) (Scheme 1). The latter was included for comparison, although no experimental KIE data are known.

(37) Frisch, M. J. T.; Trucks, G. W.; Schlegel, H. B.; Scuseria, G. E.; Robb, M. A.; Cheeseman, J. R.; Montgomery, J. A., Jr.; Vreven, T.; Kudin, K. N.; Burant, J. C.; Millam, J. M.; Iyengar, S. S.; Tomasi, J.; Barone, V.; Mennucci, B.; Cossi, M.; Scalmani, G.; Rega, N.; Petersson, G. A.; Nakatsuji, H.; Hada, M.; Ehara, M.; Toyota, K.; Fukuda, R.; Hasegawa, J.; Ishida, M.; Nakajima, T.; Honda, Y.; Kitao, O.; Nakai, H.; Klene, M.; Li, X.; Knox, J. E.; Hratchian, H. P.; Cross, J. B.; Bakken, V.; Adamo, C.; Jaramillo, J.; Gomperts, R.; Stratmann, R. E.; Yazyev, O.; Austin, A. J.; Cammi, R.; Pomelli, C.; Ochterski, J. W.; Ayala, P. Y.; Morokuma, K.; Voth, G. A.; Salvador, P.; Dannenberg, J. J.; Zakrzewski, V. G.; Dapprich, S.; Daniels, A. D.; Strain, M. C.; Farkas, O.; Malick, D. K.; Rabuck, A. D.; Raghavachari, K.; Foresman, J. B.; Ortiz, J. V.; Cui, Q.; Baboul, A. G.; Clifford, S.; Cioslowski, J.; Stefanov, B. B.; Liu, G.; Liashenko, A.; Piskorz, P.; Komaromi, I.; Martin, R. L.; Fox, D. J.; Keith, T.; Al-Laham, M. A.; Peng, C. Y.; Nanayakkara, A.; Challacombe, M.; Gill, P. M. W.; Johnson, B.; Chen, W.; Wong, M. W.; Gonzalez, C.; and Pople, J. A. *Gaussian03*, revision C.02; Gaussian, Inc.: Wallingford, CT, 2004.

(38) Lee, C.; Yang, W.; Parr, R. G. *Phys. Rev. B: Condens. Matter* **1988**, *37*, 785−789.

(39) Vosko, S. H.; Wilk, L.; Nusair, M. *Can. J. Phys.* **1980**, *58*, 1200−1211.

(40) Becke, A. D. *J. Chem. Phys.* **1993**, *98*, 5648−5652.

(41) Stephens, P. J.; Devlin, F. J.; Chabalowski, C. F.; Frisch, M. J. *J. Phys. Chem.* **1994**, *98*, 11623−11627.

(42) Hehre, W. J.; Ditchfield, R.; Pople, J. A. *J. Chem. Phys.* **1972**, *56*, 2257−2261.

(43) Andrae, D.; Haeussermann, U.; Dolg, M.; Stoll, H.; Preuss, H. *Theor. Chim. Acta* **1990**, *77*, 123−141.

(44) Andrae, D.; Haeussermann, U.; Dolg, M.; Stoll, H.; Preuss, H. *Theor. Chim. Acta* **1991**, *78*, 247−266.

(45) Schlegel, H. B. *J. Comput. Chem.* **1982**, *3*, 214−218.

(46) Schaftenaar, G.; Noordik, J. H. *J. Comput.-Aided Mol. Des.* **2000**, *14*, 123−134.

(47) Cossi, M.; Barone, V.; Cammi, R.; Tomasi, J. *J. Chem. Phys.* **1996**, *255*, 327−335.

(48) Radrich, H.; Busold, M.; Drees, M.; Strassner, T., in preparation.

(49) Saunders, M.; Laidig, K. E.; Wolfsberg, M. *J. Am. Chem. Soc.* **1989**, *111*, 8989−8994.

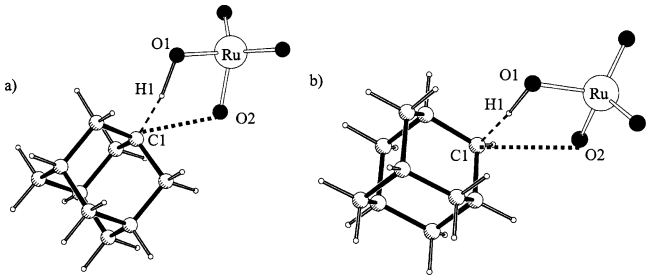

FIGURE 1. RuO_4−adamantane transition states and selected distances (Å): (a) **TS1a** ($\Delta G^{\ddagger}$ = 23.6 kcal/mol) → Ru−O1 = 1.79, Ru−O2 = 1.75, O1−H1 = 1.21, H1−C1 = 1.38, O2−C1 = 2.75; (b) **TS1b** ($\Delta G^{\ddagger}$ = 26.6 kcal/mol) → Ru−O1 = 1.80, Ru−O2 = 1.75, O1−H1 = 1.20, H1−C1 = 1.39, O2−C1 = 2.57.

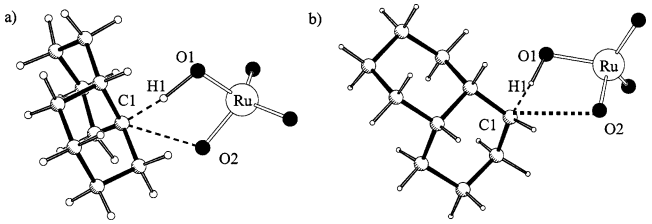

FIGURE 2. RuO_4−*cis*-decalin transition states and selected distances (Å): (a) **TS2a** ($\Delta G^{\ddagger}$ = 24.1 kcal/mol) → Ru−O1 = 1.79, Ru−O2 = 1.75, O1−H1 = 1.22, H1−C1 = 1.39, O2−C1 = 2.84; (b) **TS2b** ($\Delta G^{\ddagger}$ = 26.1 kcal/mol) → Ru−O1 = 1.80, Ru−O2 = 1.75, O1−H1 = 1.20, H1−C1 = 1.39, O2−C1 = 2.57.

From previous studies of related compounds,[23,35,36] we know that the (3+2) transition state is usually significantly preferred over the corresponding (2+2) transition state. Therefore, we restricted the study to the calculation of the (3+2) transition states, as proposed in the experimental literature. Table 1 summarizes the calculated transition-state thermodynamics together with available experimental activation data for the hydrocarbon oxidation by RuO_4 in a solution of $CCl_4/CH_3CN/H_2O$ (AN) at a temperature of 303.55 K, as well as in a solution of acetone/water (AC) at a temperature of 305.55 K. The solvation calculations were performed using the polarity of acetonitrile (AN, ϵ = 36.64) at 303.55 K and of acetone (AC, ϵ = 20.7) at 305.55 K. Gas-phase calculations were carried out at 298 and 305 K, but the different temperatures showed no effects on the ΔH_{calc}, and only little effect on the corresponding ΔG_{calc} values. (They increased by 0.1−0.2 kcal/mol for 305 K.)

With the exception of *trans*-decalin, all substrates show a barrier for the RuO_4 oxidation of a tertiary C−H bond that is about 2.5 kcal/mol less than that for the secondary bonds. The primary C−H bonds in methane obviously have to be harder to oxidize, which the calculations account for by giving an energy about 10 kcal/mol higher. For the secondary and tertiary C−H bonds in *trans*-decalin, very similar activation enthalpies and energies (within 0.5 kcal/mol) have been calculated. Compared to experimental values, the computational results are in good agreement.

The calculated geometries show comparable bond length in the transition states (Figures 1−3) for all substrates. The most significant difference between the transition-state geometries for the activation of a secondary C−H bond compared to a tertiary C−H bond is the C1−O2 distance, which is calculated to be 0.2 Å shorter for secondary C−H bond activations than for tertiary ones. The secondary interaction between C1 and O2

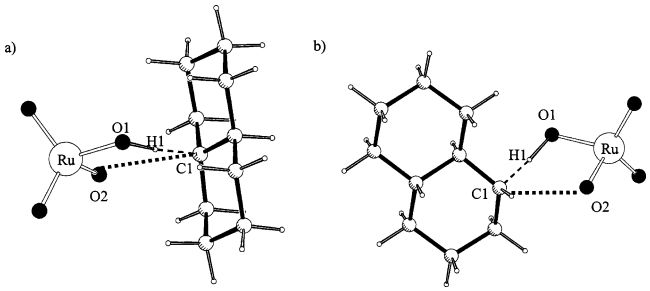

FIGURE 3. RuO_4−*trans*-decalin transition states and selected distances (Å): (a) **TS3a** ($\Delta G^{\ddagger}$ = 25.7 kcal/mol) → Ru−O1 = 1.80, Ru−O2 = 1.75, O1−H1 = 1.21, H1−C1 = 1.41, O2−C1 = 2.84; (b) **TS3b** ($\Delta G^{\ddagger}$ = 25.3 kcal/mol) → Ru−O1 = 1.79, Ru−O2 = 1.75, O1−H1 = 1.21, H1−C1 = 1.37, O2−C1 = 2.57.

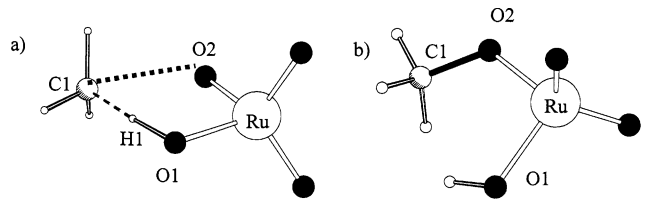

FIGURE 4. RuO_4−methane transition state, intermediate, and selected distances (Å): (a) **TS4** ($\Delta G^{\ddagger}$ = 34.6 kcal/mol) → Ru−O1 = 1.79, Ru−O2 = 1.75, O1−H1 = 1.19, H1−C1 = 1.38, O2−C1 = 2.27; (b) **IM4** (ΔG = −19.5 kcal/mol) → Ru−O1 = 1.90, Ru−O2 = 1.90, O2−C1 = 1.42.

expresses itself by a significant elongation (on average 0.05 Å) of the Ru−O2 bond compared to those Ru−O bonds not involved in the reaction (1.70 Å)

A comparison of the calculated energies shows the activation of *trans*-decalin to be a special case. The calculated differences for the two transition states **TS3a** and **TS3b** (Figure 3) propose that the reaction should lead to an activation of both bonds and product mixtures of tertiary and secondary alcohols. Unfortunately, Bakke did not report which products he obtained after workup.

Methane is well-known to be very hard to activate, which leads to the highest transition state (Figure 4) of the chosen substrates. It is also a very late transition state with an interesting secondary interaction between C1 and O2 in the transition state. This interaction has also been observed for other metal−oxo compounds. Details will be reported soon.

Experimental KIE data are available from Bakke's work; therefore we calculated the corresponding theoretical values (Table 2). Bakke observed KIEs at 305 K that are dependent on the solvent system. When they applied the Sharpless condition (a mixture of CCl_4, water, and acetonitrile), the resulting KIE was 4.8 and did not differentiate between *cis*-decalin and adamantane. In a mixture of acetone and water, a larger KIE was reported for the RuO_4-mediated oxidation of adamantane (7.8) than for *cis*-decalin (6.8). In our gas-phase calculations at 298 K, we obtained greater KIEs for adamantane (6.0) than for *cis*-decalin (5.0), which is in agreement with the experimental KIE in the latter case.

The calculated KIEs show that the activation of a tertiary C−H bond by RuO_4 is expected to show a KIE higher than that for oxidative cleavage of the corresponding secondary C−H bond. The magnitude of the KIE might also be influenced by the almost linear geometry in the proximity of the transition state, as can be seen from the IRC data, but clearly no secondary KIEs are necessary to explain the large effect.

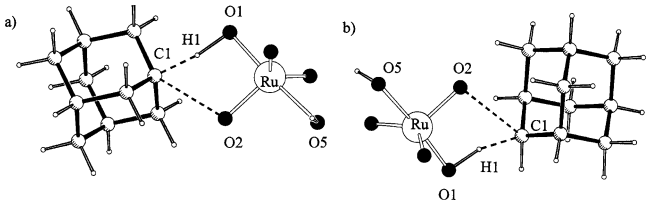

FIGURE 5. $RuO_4(OH)^-$−adamantane transition states and selected distances (Å): (a) **TS5a** ($\Delta G^‡$ = 23.5 kcal/mol) → Ru−O1 = 1.87, Ru−O2 = 1.75, O1−H1 = 1.16, H1−C1 = 1.39, O2−C1 = 2.60, O5−Ru = 2.07; (b) **TS5b** ($\Delta G^‡$ = 27.8 kcal/mol) → Ru−O1 = 1.88, Ru−O2 = 1.76, O1−H1 = 1.13, H1−C1 = 1.43, O2−C1 = 2.78, O5−Ru = 2.07.

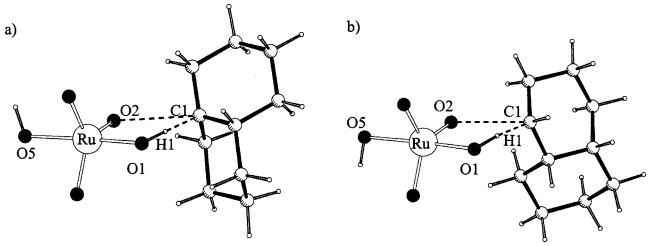

FIGURE 6. $RuO_4(OH)^-$−*cis*-decalin transition states and selected distances (Å): (a) **TS6a** ($\Delta G^‡$ = 22.7 kcal/mol) → Ru−O1 = 1.88, Ru−O2 = 1.75, O1−H1 = 1.16, H1−C1 = 1.41, O2−C1 = 2.71, O5−Ru = 2.07; (b) **TS6b** ($\Delta G^‡$ = 26.6 kcal/mol) → Ru−O1 = 1.87, Ru−O2 = 1.75, O1−H1 = 1.16, H1−C1 = 1.39, O2−C1 = 2.61, O5−Ru = 2.07.

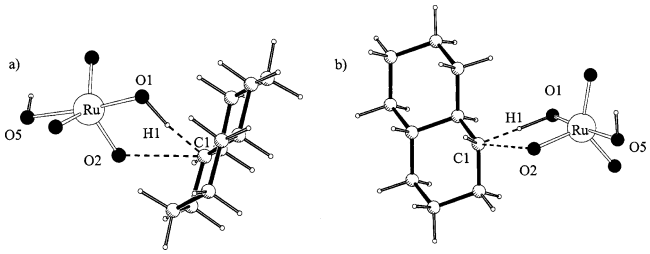

FIGURE 7. $RuO_4(OH)^-$−*trans*-decalin transition states and selected distances (Å): (a) **TS7a** ($\Delta G^‡$ = 23.2 kcal/mol) → Ru−O1 = 1.88, Ru−O2 = 1.75, O1−H1 = 1.15, H1−C1 = 1.43, O2−C1 = 2.72, O5−Ru = 2.06; (b) **TS7b** ($\Delta G^‡$ = 23.5 kcal/mol) → Ru−O1 = 1.87, Ru−O2 = 1.75, O1−H1 = 1.16, H1−C1 = 1.39, O2−C1 = 2.51, O5−Ru = 2.07.

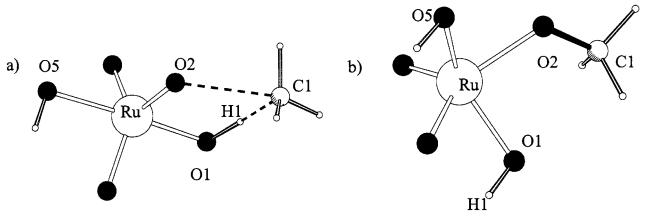

FIGURE 8. $RuO_4(OH)^-$−methane transition state, intermediate, and selected distances (Å): (a)**TS8** ($\Delta G^‡$ = 28.4 kcal/mol) → Ru−O1 = 1.87, Ru−O2 = 1.75, O1−H1 = 1.15, H1−C1 = 1.40, O2−C1 = 2.33, O5−Ru = 2.08; (b) **IM8** (ΔG = −40.4 kcal/mol) → Ru−O1 = 1.94, Ru−O2 = 1.97, O2−C1 = 1.40, O5−Ru = 1.93.

We also calculated the corresponding intermediates of the C−H activation reactions (Table 3). Their geometries and coordinates are given in the Supporting Information, with the exception of the methane intermediate, which is shown in Figure 4. These intermediates are proposed to be precursors of the general formula $Ru(OH)(OR)O_2$ that yield the corresponding alcohol upon oxidative workup. It is interesting to note that on this level of theory the reaction of a secondary C−H bond in *cis*-decalin is slightly more exergonic than the reaction of a tertiary bond. Therefore, the formation of *cis*-1-decalin is only kinetically favored, whereas the oxidation of a tertiary C−H bond in adamantane is both thermodynamically and kinetically favored. For *trans*-decalin, no clear thermodynamic and kinetic distinction is possible between secondary and tertiary bond oxidation. From our calculations, *trans*-1-decanol and *trans*-2-decanol should be found as products.

Mayer and co-workers very recently published an experimental study on the OsO_4 oxidation of alkanes. They showed that the oxidation is pH dependent, and under basic conditions, they proposed the anion $OsO_4(OH)^-$ to be the active species. As RuO_4 and OsO_4 show comparable reactivities, it should be possible that a similar species $RuO_4(OH)^-$ is formed under basic conditions, though we have to keep in mind that RuO_4 forms ruthenate salts above pH 9. The energies of transition states and intermediates together with the theoretical KIE for $RuO_4(OH)^-$ are summarized in Table 4.

All reported energy values are relative to the educt pair $RuO_4(OH)^-$/alkane. On the basis of gas-phase calculations, the formation of $RuO_4(OH)^-$ is highly exergonic, with a free energy of −81.2 kcal/mol.

When comparing the energies of Tables 1, 3, and 4, we find that the influence of an anionic active species is more distinct at intermediates than at transition states. The energies of all adducts are around 20−30 kcal/mol more exergonic than in the case of ruthenium tetraoxide, whereas the transition states differ by only 2−3 kcal/mol. The calculated kinetic isotope effects are slightly higher (0.2−0.5) compared to the values calculated for the RuO_4 oxidations.

All transition states seem to be later on the energy surface than in the case of RuO_4, and all transition states show longer Ru−O1 distances and shorter O1−H1 bonds (see Figures 5−8).

Energetically, the differences for the activation of secondary and tertiary C−H bonds are comparable to the RuO_4 case, just a little larger (around 4 kcal/mol for the transition states). Also, for $RuO_4(OH)^-$, the difference for *trans*-decalin is significantly smaller, but for the anionic $RuO_4(OH)^-$, the tertiary C−H bond has a lower barrier (of 0.3 kcal/mol).

One example of a ruthenate intermediate is shown in Figure 8b. The greater stability of these adducts is certainly due to the OH ligands, which appear to have formed a real Ru−O bond (1.93 Å).

Conclusion

Our computational study reveals that the RuO_4-catalyzed activation of alkane C−H bonds follows a (3+2) pathway that is in good agreement with experimental results from earlier work of Bakke. Enthalpies and free energies show only small differences between experimental and theoretical values (less than 1 kcal/mol for ΔH or less than 3 kcal/mol for ΔG). The proposed mechanism is confirmed by the evaluation of experimental and theoretical KIEs. Gas-phase kinetic isotope effects were calculated to be in the range of 5.0−6.0 for tertiary C−H bond oxidations.

We also simulated basic conditions in which the (hypothetic) hydroxide adduct $RuO_4(OH)^-$ serves as the active species. The influence on the transition states and therefore on the observed KIEs is minimal; mostly the ruthenate intermediates would be affected and stabilized from this additional ligand at the

ruthenium center. On the basis of our calculations, both species could serve as the active catalyst.

Acknowledgment. The authors are grateful for the donation of memory chips by Infineon, and for financial support by the Fonds der Chemischen Industrie. T.S. thanks M.D. for the cover design.

Supporting Information Available: All *xyz* coordinates are provided in the Supporting Information, together with structures of the calculated intermediates and tables for the relative electronic energies (ΔE). This material is available free of charge via the Internet at http://pubs.acs.org.

JO051521D